

Measurements of the Einstein relation in doped and undoped molecular thin films

O. Tal,^{1,*} I. Epstein,¹ O. Snir,¹ Y. Roichman,^{2,†} Y. Ganot,² C. K. Chan,³ A. Kahn,³ N. Tessler,² and Y. Rosenwaks¹

¹*School of Electrical Engineering-Physical Electronics, Tel Aviv University, Tel Aviv 69978, Israel*

²*Department of Electrical Engineering, Technion Israel Institute of Technology, Haifa 32000, Israel*

³*Department of Electrical Engineering, Princeton University, Princeton, New Jersey 08544, USA*

(Received 13 February 2008; published 2 May 2008)

We present the Kelvin probe force microscopy measurements of the Einstein relation, i.e., the relation between the diffusion coefficient of charge carriers and their mobility, in undoped and doped disordered organic thin films. The theoretical prediction of a large deviation of the Einstein relation from its classical value is verified and attributed to the energy distribution of the density of states. The results are explained in the context of degeneracy effects on the transport in disordered organic thin films, and their implications for organic-based devices are discussed.

DOI: [10.1103/PhysRevB.77.201201](https://doi.org/10.1103/PhysRevB.77.201201)

PACS number(s): 72.80.Le, 71.23.Cq, 72.20.Ee

The Einstein relation (ER) is the relation between two fundamental transport parameters, the diffusion coefficient D and the mobility μ of charge carriers. Considerable attention has been recently paid to both experimental and theoretical studies of the ER in organic disordered semiconductors (DSs).¹⁻⁴ A generalized ER can be derived by using a general charge carrier energy distribution and can be written for holes as⁵

$$D/\mu = -p[qd\rho/dE_{fp}]^{-1}, \quad (1)$$

where q is the elementary charge, E_{fp} is the hole quasi-Fermi level, and p is the hole concentration given by

$$p = \int_{-\infty}^{\infty} g(E)f_{FD}^h(E)dE. \quad (2)$$

Here, $g(E)$ is the density of states (DOS) and $f_{FD}^h(E)$ is the Fermi-Dirac distribution for holes.

It has been shown using calculations based on the shape of the DOS¹⁻³ that deviations from the classical ER, in which $\eta=1$ in $D/\mu=\eta(kT/q)$, are expected for DS under equilibrium¹ as well as nonequilibrium conditions.⁶ This deviation has substantial implications on the performance of electronic devices based on DS in general and disordered organic films in particular. Indeed, highly dispersive photocurrent in time-of-flight measurements of hydrogenated amorphous silicon,⁷ the broad rise of the turn-on current in organic light emitting diodes,¹ and the temperature dependence of the ideality factor in organic p - n homojunctions^{4,8} can be explained by ER deviations from kT/q for disordered materials. Deviations were also found in degenerate crystalline inorganic semiconductors.⁹ In DS, with tail states penetrating deep into the energy gap, degeneracy effects are even more pronounced,¹⁰ and it has been shown by calculations that, due to high degeneracy, the deviation from the conventional ER very sensitively depends on the shape of the DOS.¹¹ However, to the best of our knowledge, there are no reported measurements of the ER in organic semiconductors that directly verify the predicted deviations from kT/q .

We present here the measurements of the ER as a function of the quasi-Fermi energy (E_{fp}) and charge concentration in undoped and doped disordered organic thin films. The ER is

obtained from the Kelvin probe force microscopy (KPFM) measurements taken across operating organic thin film transistors (OTFTs). Our results confirm that the ER deviates from the classical value and reveals a rich behavior, which is ascribed to the specific shape of the DOS in both the doped and the undoped materials.

The measurements were conducted on a bottom contact OTFTs that consist of a heavily doped p -type silicon gate electrode, a thermally grown 90 nm silicon oxide gate insulator, and 50 nm thick gold strips evaporated on the oxide to form source and drain electrodes separated by 8 or 16 μm . Thin films (10 nm) of undoped N,N' -diphenyl- N,N' -bis(1-naphthyl)-1,1'-biphenyl-4,4'-diamine (α -NPD) and α -NPD doped with tetrafluorotetracyanoquinodimethane (F_4 -TCNQ) ($\sim 0.1\%$) were deposited on the substrates by sublimation in an ultrahigh vacuum chamber. The transistors were then transported under nitrogen atmosphere to a nitrogen glove box (<2 ppm H_2O) in which the KPFM (CP II-Veeco, Inc., atomic force microscopy) measurements were conducted. A semiconductor parameter analyzer (Agilent 4155C) was used to control the gate voltage, with respect to the grounded source and drain electrodes, and monitor the drain, source, and gate electrode currents. The contact resistance, leakage currents, and shifts of the threshold voltage^{12,13} due to continuous voltage application were negligible in the measured transistors. The threshold voltage shifts (-0.1 and -0.2 V in total for the undoped and doped samples) were taken into consideration in the analysis.

The hole concentration in the transistor channel was controlled by applying a gate-source voltage (V_{GS}) while measuring the local vacuum level shift with the KPFM (the method is described in detail in Refs. 14 and 15). Up to a given V_{GS} , the molecular levels are shifted rather than bent across the 10 nm thin organic film,¹⁴ and the shift of the energy levels (V_L) for different V_{GS} with respect to the level position at $V_{GS}=V_t$ (the transistor threshold voltage) can be directly measured by KPFM using¹⁵ $V_L(x)\equiv\text{CPD}(x)-\text{CPD}_t(x)$, where x is the lateral coordinate along the channel between source and drain, CPD is the contact potential difference, and CPD_t is the CPD measured at $V_{GS}=V_t$.

In the V_{GS} range where the charge concentration is homogeneously distributed across the width of the organic film,¹⁴ the hole concentration can be extracted using

$$p(x) = -(C_{ox}/qd_{org})[V_{GS} - V_t - V_L(x)], \quad (3)$$

where C_{ox} is the silicon oxide capacitance and d_{org} is the thin film width. Inserting Eq. (3) into the generalized form of ER [Eq. (1)] gives the ER from the KPFM measurements,

$$D_h/\mu_h(x) = -q^{-1}p(x)/[dp(x)/dV_L(x)] \\ = [V_{GS} - V_t - V_L(x)]/\{1 - [dV_{GS}/dV_L(x)]\}, \quad (4)$$

where $dV_L(x) = -dE_{fp}(x)/q$; the extraction of the ER using Eq. (4) is based only on the measured shift of the energy levels (V_L), so it can be regarded as a direct ER measurement.¹⁶ Our measurements are conducted at $V_{DS} = 0$ V for different V_{GS} ; hence, the ER can be obtained as a function of the injected carrier concentration and of the shift of E_{fp} from its position at $V_{GS} = V_t$. Each measurement is conducted a long enough time after setting a new V_{GS} voltage, thus I_{DS} is negligibly small at $V_{DS} = 0$ V.

In order to study the correlation between the ER and the DOS, the hole concentration and the energy level shift can also be used to calculate the hole DOS using¹⁴

$$g(qV_L(x)) = q^{-1}[dp(x)/dV_L(x)] \\ = [C_{ox}/(d_{org}q^2)](\{d[V_{GS}(x) - V_t]/dV_L(x)\} - 1). \quad (5)$$

The ER is affected by the shape of the DOS via the charge concentration and the position of E_{fp} through Eqs. (1) and (2),

$$D_h/\mu_h = q^{-1} \left(\int_{-\infty}^{\infty} g(E)f_{FD}(E)dE \right) / \left(\int_{-\infty}^{\infty} g(E) \right. \\ \left. \times [df_{FD}(E)/dE_{fp}]dE \right), \quad (6)$$

and for $g(E)$ much wider than $df_{FD}(E)/dE_{fp}$,

$$D_h/\mu_h \cong p/qg(E_{fp}). \quad (7)$$

We first focus on ER measurements of doped α -NPD:F₄-TCNQ(0.1%) thin film transistor. Figure 1(a) shows the measured DOS (circles), an analytical fit for the DOS (solid curve), and the calculated charge density using Eq. (2) (squares) as a function of the quasi-Fermi energy. $E_{fp} = 0$ is defined throughout the Rapid Communication as the energy at which the level shift is zero, i.e., $V_L = 0$. The DOS fit in Fig. 1(a) can be divided into two main regions: a commonly used model of an exponential tail for $0 \text{ eV} > E > -0.16 \text{ eV}$ (Ref. 17) and a sum of two Gaussians for $E < -0.16 \text{ eV}$. The latter is based on a model presented by Arkhipov *et al.*,¹⁸ which was fitted to the baseline of the DOS (ignoring the appearance of the sharp peaks), with variance of $0.08 \pm 0.01 \text{ eV}$. The peak distribution on the DOS baseline was found to be reproducible at different lateral locations and for different measurement times. We tentatively attribute these peaks to multiple dopant induced energy levels introduced by different dopant and host molecule configurations or dopant aggregates of different sizes (see Ref. 14 for a detailed analysis of the DOS structure).

Figure 1(b) shows the ER obtained by plugging the mea-

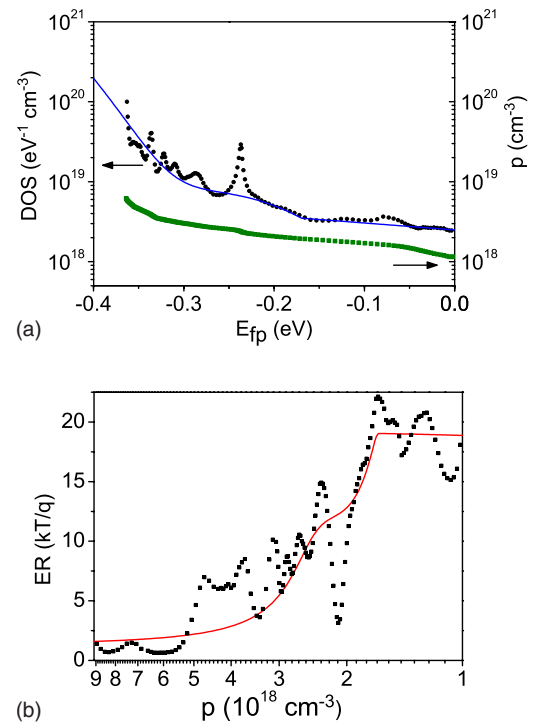


FIG. 1. (Color online) (a) Measured DOS (circles), analytical fit of the DOS (solid curve), and charge density measured using Eq. (2) (squares) as a function of the quasi-Fermi energy for a doped α -NPD:F₄-TCNQ thin film. (b) Measured ER obtained from KPFM and Eq. (4) (squares) and calculated using Eq. (6) (solid curve) as a function of charge density for a doped α -NPD:F₄-TCNQ thin film.

sured $dV_{GS}/dV_L(x)$ into Eq. (4) (squares), while the solid curve reveals the general behavior of the ER; the later was obtained by applying Eq. (6) to the DOS fit [solid curve in Fig. 1(a)]. The general shape of the ER can be understood in terms of Eq. (7) by examining the dependence of the DOS and the charge density on the position of the quasi-Fermi level shown in Fig. 2. For $0 \geq E_{fp} \geq -0.16 \text{ eV}$ ($1.71 \times 10^{17} \leq p \leq 1.91 \times 10^{18} \text{ cm}^{-3}$), the relative change in the DOS is very similar to the change in the charge density with the

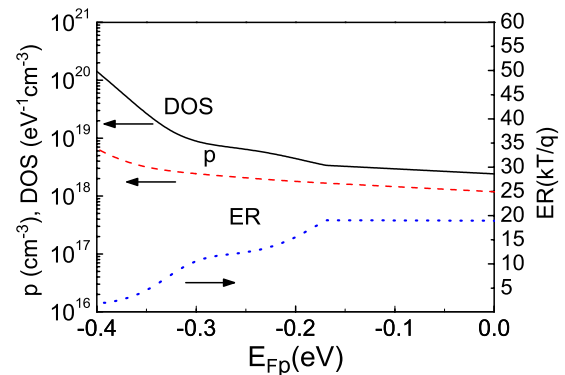


FIG. 2. (Color online) Analytical fit of the DOS presented in Fig. 1(a) (solid curve, left scale), calculated charge density (dashed curve, left scale) using Eq. (2), and ER (dotted curve, right scale) as a function of the quasi-Fermi energy obtained by Eq. (6).

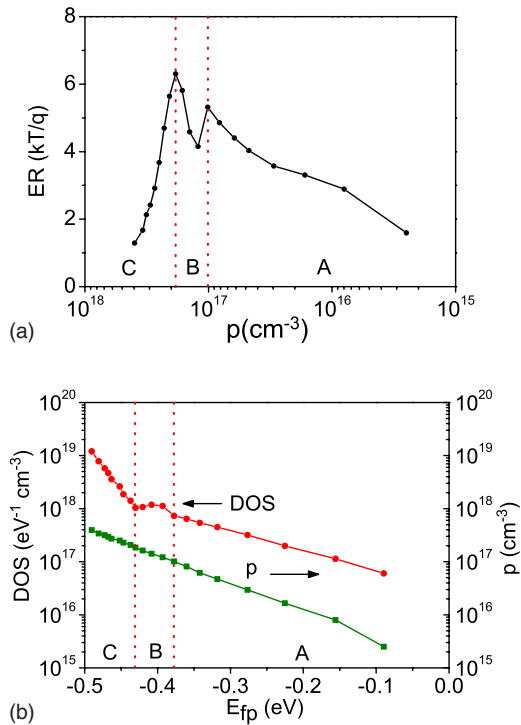


FIG. 3. (Color online) (a) Measured ER as a function of charge density for undoped α -NPD (b) Measured DOS (circles, left scale) and charge density (squares, right scale) measured using Eq. (3) as a function of the quasi-Fermi energy for undoped α -NPD.

result that the ER is roughly constant. In this range, the ER is considerably higher ($\sim 19kT/q$) than its classical value. Such a high ER is an indication of a high charge concentration in comparison to the available DOS at certain energy [see Eq. (7)]. This can result from a relatively low state density tail penetrating into the forbidden gap, as indeed appears in Fig. 1(a).

The decrease in ER for $E_{fp} < -0.16$ eV ($p > 1.91 \times 10^{18}$ cm $^{-3}$) is due to the transition of the DOS from an exponential to a multi-Gaussian shape; since the DOS increases faster than the charge density, the ER decreases [Eq. (7)]. The transition between the two Gaussian features in the DOS is manifested as a shoulder in the ER at $E_{fp} \cong -0.3$ eV ($p \cong 3.02 \times 10^{18}$ cm $^{-3}$). The high value of the measured ER, as compared to the classical value, is not surprising when considering the well-known broadening effect of doping on the DOS in organic thin films.¹⁸ Consequently, the DOS includes a tail of states in forbidden gap that can lead to high ER values and a complex behavior as a function of charge concentration.

The measured ER as a function of the charge density is shown in Fig. 3(a) for undoped α -NPD. The ER is larger than kT/q for the whole range of the measured charge concentration, and its dependence on the charge density can be explained by considering three different regions: ER increasing for $p < 1.01 \times 10^{17}$ cm $^{-3}$ [region A in Fig. 3(a)], followed by a depression for $1.01 \times 10^{17} \leq p \leq 1.85 \times 10^{17}$ cm $^{-3}$ (region B), and ER decreasing for $p > 1.85 \times 10^{17}$ cm $^{-3}$ (region C). Figure 3(b) shows the measured DOS (circles), and the measured charge density as a function of E_{fp} (squares),

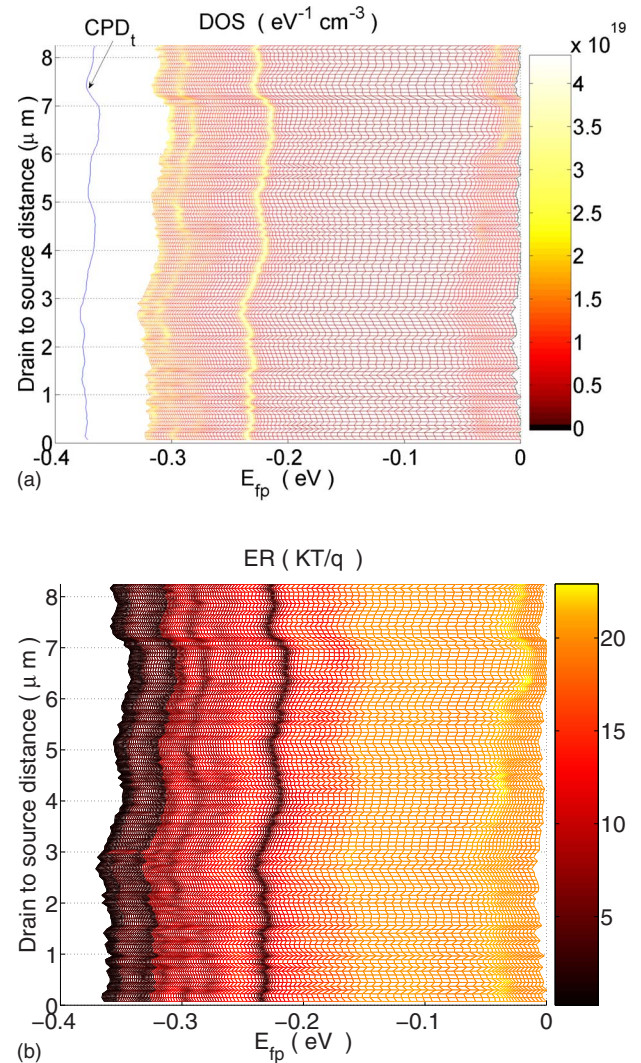


FIG. 4. (Color online) (a) DOS (color axis) measured throughout the channel (y axis) as a function of the quasi-Fermi energy (x-axis) for a doped α -NPD:F₄-TCNQ thin film transistor. (b) Measured ER (color axis) throughout the channel (y axis) as a function of quasi-Fermi energy (x axis) for a doped α -NPD:F₄-TCNQ thin film transistor.

where regions A, B, and C are defined as in Fig. 3(a). As the charge concentration is approximately an integral on the DOS up to E_f , it almost exponentially increases without substantial differences across the three regions, while the DOS has a different behavior in each region. Therefore, according to Eq. (7), the fine structure of the DOS distribution determines the shape of the ER curve [see Eq. (7)]. The ER behavior for the undoped sample demonstrates the sensitivity to the rich DOS structure even in the absence of DOS broadening by doping. Near the limit of the measured energy region (most negative energy), the transition from the relatively flat DOS distribution to a steeper distribution decreases the ER deviation from kT/q . Note that the ER derived here can be considered under equilibrium conditions. However, the generalized ER that is defined for nonequilibrium conditions, as the time-dependent D/μ ratio commonly measured by time of flight,⁷ is expected to follow the same

trend: higher ER due to lower DOS and sensitivity to the DOS fine structure.

The origin for the ER deviation from kT/q can be understood by considering the different effects of energetic disorder on charge diffusion and drift. Diffusion describes a charged carrier motion that tends to eliminate any spatial difference in their density. Accordingly, the flux of carriers in diffusion is from a high carrier density region to low carrier density regions. So the target sites for the moving carriers are most likely empty. In contrast, carrier drift is dictated by the direction of the electric field. Thus, under equilibrium conditions, the net flux of carriers in drift, which cancels the diffusion flux, is from low carrier density (relatively empty) region to high carrier density (relatively filled) region, so the drift current depends on the probability of the target site to be occupied. In amorphous organic films, where the DOS does not considerably increase with energy (as was shown here), the charge density rises to a level where the DOS can become significantly filled. Consequently, the drift current is suppressed more than the diffusion current, leading to a rise in the ER.

Scanning KPFM allows a determination of the DOS and ER throughout the organic field effect transistor channel with high lateral resolution. Figure 4(a) shows the DOS measured across the transistor channel for doped α -NPD and Fig. 4(b) presents the corresponding ER. The peak sequence observed in the DOS and the corresponding deeps in the ER located at around 0.24 and 0.3 eV preserve their general structure along the channel, despite $\sim \pm 0.01$ eV energetic fluctuation of the entire sequence. Such behavior indicates on the fluctuations in the total potential energy (observed also in the CPD profile taken at $V_{GS}=V_t$). Since the KPFM resolution is estimated to

be tens of nanometers, the observed lateral energetic disorder is not likely to indicate on energetic fluctuations near individual dopants. However, the observed energetic fluctuations can stem from variation in the intermolecular spacing and orientation.

The large ER found here and its sensitivity to the charge concentration or the Fermi energy position is of utmost importance in organic electronic devices. For example, it has been shown^{4,9} that the p - n diode ideality factor is proportional to η ; this implies that unlike with inorganic semiconductors, doping of organic materials in p - n junctions will have a much larger effect on carrier transport. In particular, it will lead to an increased diffusion current in organic photovoltaic cells; consequently, the number of charge carriers that are lost by recombination will decrease, and the charge collection improved.

In conclusion, we have measured the ER as a function of charge concentration in both undoped and doped disordered organic thin films. It was found that the ER significantly deviates from kT/q and is sensitive to changes in the DOS. Such high ER at the Fermi level energy is an indication of diffusion controlled transport in organic materials and devices. A high lateral resolution DOS and ER maps showed that the main features that appear throughout the channel are correlated with local changes in the channel surface potential.

This research was generously supported by the US-Israel Binational Science Foundation (BSF) under Grant No. 2000-092. A.K. also acknowledges partial support by the NSF (DMR-0408589) and N.T. acknowledges partial support by the Israel Science Foundation.

*Present address: Leiden Institute of Physics, Leiden University, 2300 RA Leiden, Netherlands.

[†]Present address: Department of Physics, New York University, New York 10003, USA.

¹Y. Roichman and N. Tessler, *Appl. Phys. Lett.* **80**, 1948 (2002).

²T. H. Nguyen and S. K. O'Leary, *J. Appl. Phys.* **98**, 076102 (2005).

³Y. Peng *et al.*, *Appl. Phys. A: Mater. Sci. Process.* **86**, 225 (2007).

⁴K. Harada, A. G. Werner, M. Pfeiffer, C. J. Bloom, C. M. Ellio, and K. Leo, *Phys. Rev. Lett.* **94**, 036601 (2005).

⁵S. M. Sze, *Physics of Semiconductor Devices*, 2nd ed. (Wiley, New York, 1981).

⁶R. Richert, L. Pautmeier, and H. Bässler, *Phys. Rev. Lett.* **63**, 547 (1989); V. I. Arkhipov and G. J. Adriaenssens, *J. Phys.: Condens. Matter* **8**, 7909 (1996).

⁷Q. Gu, E. A. Schiff, S. Grebner, F. Wang, and R. Schwarz, *Phys. Rev. Lett.* **76**, 3196 (1996).

⁸N. Tessler and Y. Roichman, *Org. Electron.* **6**, 200 (2006).

⁹D. Ritter, E. Zeldov, and K. Weiser, *Phys. Rev. B* **38**, 8296 (1988); H. Kroemer, *IEEE Trans. Electron Devices* **25**, 850 (1978).

¹⁰T. H. Nguyen and S. K. O'Leary, *J. Appl. Phys.* **88**, 3479 (2000).

¹¹Y. Q. Peng, S. Sun, and C. A. Song, *Mater. Sci. Semicond. Process.* **8**, 525 (2005).

¹²G. Horowitz *et al.*, *Adv. Funct. Mater.* **14**, 1069 (2004).

¹³O. Tal *et al.*, *Appl. Phys. Lett.* **88**, 043509 (2006).

¹⁴O. Tal, Y. Rosenwaks, Y. Preezant, N. Tessler, C. K. Chan, and A. Kahn, *Phys. Rev. Lett.* **95**, 256405 (2005).

¹⁵O. Tal and Y. Rosenwaks, *J. Phys. Chem. B* **110**, 25521 (2006).

¹⁶When further increases, the ER is abruptly reduced to zero beyond the valid range of Eqs. (2)–(5), thus measurements of faulty ER are easily avoided.

¹⁷M. C. J. M. Vissenberg and M. Matters, *Phys. Rev. B* **57**, 12964 (1998).

¹⁸V. I. Arkhipov, P. Heremans, E. V. Emelianova, and H. Bassler, *Phys. Rev. B* **71**, 045214 (2005).